doi:10.1093/scan/nsr047 SCAN (2012) 7, 588–595

Changes in cortical morphology resulting from long-term amygdala damage

Aaron D. Boes,[1,*] Sonya Mehta,[2,3,*] David Rudrauf,[4,5] Ellen Van Der Plas,[6] Thomas Grabowski,[2,3] Ralph Adolphs,[7] and Peg Nopoulos[6]

[1]Department of Pediatric Neurology, Massachusetts General Hospital, Harvard University, [2]Department of Radiology, [3]Department of Neurology, University of Washington, Seattle, WA, [4]Department of Neurology, [5]Department of Radiology, [6]Department of Psychiatry, University of Iowa Carver College of Medicine, Iowa City, IA and [7]Division of Humanities and Social Sciences, California Institute of Technology, Pasadena, CA, USA

The amygdala's contribution to emotion, cognition and behavior depends on its interactions with subcortical and cortical regions. Amygdala lesions result in altered functional activity in connected regions, but it is not known whether there might be long-term structural sequelae as well. We hypothesized that developmental bilateral amygdala lesions would be associated with specific gray matter morphometric abnormalities in the ventromedial prefrontal cortex (vmPFC), anterior cingulate cortex (ACC) and the ventral visual stream. We conducted regions of interest and vertex-based analyses of structural MRI data acquired in two patients with long-standing focal bilateral amygdala lesions (S.M. and A.P.), compared to gender- and age-matched healthy comparison subjects. Both patients showed significant proportional increases in gray matter volume of the vmPFC. Cortical thickness was increased in the vmPFC and ACC and decreased in the ventral visual stream. There were no morphometric changes in dorsolateral prefrontal cortex or dorsal visual stream cortices. These findings support the hypothesis that cortical regions strongly connected with the amygdala undergo morphometric changes with long-standing amygdala damage. This is the first evidence in humans of the remote alteration of brain morphology in association with amygdala lesions, and will help in interpreting the structural and functional consequences of amygdala pathology in neuropsychiatric disorders.

Keywords: amygdala; lesions; morphometry; plasticity; prefrontal cortex; ventromedial

INTRODUCTION

The amygdala plays a critical modulatory role in a large range of cognitive functions and behaviors, ranging from attention to memory and decision-making, especially for emotionally arousing or socially relevant stimuli. The amygdala accomplishes this role through a vast network of cortical and subcortical connections. Connectivity has been investigated using tracer studies in the monkey and MRI-based techniques such as diffusion tensor imaging (DTI) and blood oxygenation level dependent (BOLD) coherence in humans. [For comprehensive review, see (Aggleton, 2000; Whalen and Phelps, 2009)].

The ventromedial prefrontal cortex (vmPFC) and anterior cingulate cortex (ACC) have robust amygdala connections (Ghashghaei, Hilgetag, and Barbas, 2007; Morecraft *et al.*, 2007). These connections are supported in humans by DTI (Cohen *et al.*, 2008; Johansen-Berg *et al.*, 2008) and functional connectivity studies showing correlated amygdala and vmPFC/ACC activity during emotion processing tasks (Cohen *et al.*, 2008; Stein *et al.*, 2007). Damage to these structures or disruption of the connections between them often leads to deficits in emotion processing with co-occurring impairments in decision making and social behavior (Gaffan *et al.*, 1993; Bechara *et al.*, 2003). A pattern of reduced structural and functional connectivity is also seen in association with certain genetic polymorphisms (5HTTLPR) that predispose to psychiatric illness (Pezawas *et al.*, 2005). Notably, projections from the amygdala to the prefrontal cortex are considerably denser to orbital and medial regions, and only very light to dorsolateral and polar regions (Porrino *et al.*, 1981; Amaral and Price, 1984; Barbas and De Olmos, 1990; Carmichael and Price, 1995), whereas ACC connectivity includes ventral and caudal sectors (Ghashghaei *et al.*, 2007). This pattern of connectivity motivated one component of our hypothesis: that amygdala lesions should impact the ACC and vmPFC more than dorsal, lateral and anterior sectors of the prefrontal cortex (PFC).

The amygdala also has reciprocal connections with sensory association cortices, particularly with visual cortices in primates (Amaral and Price, 1984). The higher order ventral visual stream association cortices in the inferior temporal lobe project to the amygdala (Turner *et al.*, 1980). In turn, the amygdala sends excitatory projections along the entire rostral–caudal extent of the ventral visual stream (Iwai and Yukie, 1987; Amaral *et al.*, 2003; Freese and Amaral, 2005,

Received 7 November 2010; Accepted 22 June 2011
Advance Access publication 6 September 2011

This research was supported in part by the following grants: NIH NS 019632. The authors thank Douglas Langbehn for his guidance in the statistical analysis. The authors also thank Hans Johnson, Greg Harris and Nick Jones for technical support.

Correspondence should be addressed to Ralph Adolphs, California Institute of Technology, Pasadena, CA 91125, USA. E-mail: radolphs@hss.caltech.edu

*These authors contributed equally to this work.

2006). This feedback may amplify cortical processing of emotionally salient visual stimuli, such that important objects in the environment are preferentially attended to (Adolphs and Spezio, 2006; Rudrauf *et al.*, 2008). Functional magnetic resonance imaging (FMRI) studies support this hypothesis by demonstrating enhanced activation of the amygdala co-occurring with the lateral occipital and fusiform cortices when emotional content is visually displayed (Vuilleumier and Driver, 2007). As with the amygdala's projections to sectors of the prefrontal cortex, there are clear regional differences: the amygdala projects heavily to temporal cortices in the ventral visual stream (concerned with object recognition and memory) (Amaral and Price, 1984; Amaral *et al.*, 2003; Freese and Amaral, 2006), but there is essentially no connectivity between the amygdala and parietal cortices (Stefanacci and Amaral, 2000, 2002) (there are no known connections from parietal cortex to the amygdala at all, and only a very light projection reported from the amygdala to parietal area 7; (Amaral and Price, 1984). While the amygdala's projections to temporal visual cortex are massive ipsilaterally, there is even a fainter contralateral projection as well (Iwai and Yukie, 1987). This pattern of connectivity with visual cortices motivated the second component of our hypothesis: that amygdala lesions should impact temporal cortices in the ventral visual stream more than parietal cortices in the dorsal visual stream.

The aforementioned anatomical studies have ushered in a new line of investigation that combines the lesion method with functional imaging, showing causal effects of amygdala dysfunction at connected cortical regions. Subjects with bilateral amygdala damage (the participants in the current study) each showed profoundly reduced BOLD activation in the vmPFC while performing a reward learning tasks that normally activates this region (Hampton *et al.*, 2007). Subjects with unilateral amygdala damage showed a lack of BOLD signal modulation in ventral temporal cortex on the affected side when viewing fearful face stimuli (Vuilleumier *et al.*, 2004). While these studies document clear functional effects of amygdala damage on distal cortical targets, it remains an open question whether amygdala lesions might also result in long-term structural changes.

Here, we investigated cerebral cortex morphology in subjects with long-standing developmental bilateral amygdala damage. We hypothesized altered cerebral cortex volume and thickness in regions with extensive connections to the amygdala, including the vmPFC, ACC and ventral visual pathway. In contrast, we hypothesized that regions less connected with the amygdala would be structurally within normal limits, including the dorsolateral prefrontal cortex (DL PFC) and dorsal visual stream.

MATERIALS AND METHODS

Participants

Two female participants, S.M. and A.P., with rare long-standing, focal bilateral amygdala damage resulting from Urbach–Wiethe disease, participated in the study. Both are right-handed and have normal performance on standard neuropsychological tests of perception, language, memory and IQ that have been reported in detail previously (Buchanan *et al.*, 2009). They live independently and show no evidence of psychopathology; neither meets criteria for a personality disorder or other psychiatric diagnosis (Buchanan *et al.*, 2009). S.M. is a 44-year-old woman with a high-school education. She has complete bilateral amygdala damage including some damage to subjacent white matter with minor anterior entorhinal cortex involvement. A.P. is a 23-year-old woman with a college education. She has bilateral amygdala lesions occupying ~50% of the amygdala volume without involving surrounding tissue. The hippocampus is unaffected in both subjects. The extent of the amygdala lesions is further demonstrated in Supplementary Figure S1. More extensive information regarding the demographic, emotional and neuropsychological profiles of S.M. and A.P. as well as images of their brain lesions have been reported elsewhere in detail (Tranel and Hyman, 1990; Adolphs *et al.*, 1994, 1995; Tranel *et al.*, 2006; Hampton *et al.*, 2007; Buchanan *et al.*, 2009). Given what is known about Urbach–Wiethe disease, it is likely that both patients acquired amygdala lesions sometime in childhood or early adolescence. There is a growing consensus that the amygdala lesions resulting from Urbach–Wiethe disease form around the age of 10 years in most individuals (Aroni *et al.*, 1998; Staut and Naidich, 1998; Appenzeller *et al.*, 2006). Additional information describing the lesion subjects and the comparison groups is provided in Table 1. For S.M., we used MRI scans from three separate time points at ages 33, 37 and 42 years. For A.P., we had a single scan available from the age of 19 years. For each of these four target scans, we selected an age- and gender-matched healthy comparison group from a pre-existing database of MRI images collected in the Department of Neurology at the University of Iowa. All data were acquired on the same scanner, and each comparison group was matched to their respective target scan for MR pulse sequence and major hardware/software scanner upgrades.

Table 1 Descriptive subject information

Comparison groups	*n*	Age	Age range (years)
AP_{19}	1	19	–
AP_{19} comparison	57	22.61 (1.49)	19–24
SM_{33}	1	33	–
SM_{33} comparison	16	32.06 (3.23)	28–38
SM_{37}	1	37	–
SM_{37} comparison	20	34.55 (1.90)	32–38
SM_{42}	1	42	–
SM_{42} comparison	19	42.37 (2.01)	40–47

Subscripts in column 1 refer to the age of S.M. and A.P. Mean and standard deviation is shown for comparison groups.

MRI acquisition and processing

High-resolution T1-weighted images were acquired for each subject on a 1.5 T GE LX CV/i Signa scanner. A detailed description of the acquisition sequences and data averaging procedure can be found in the Supplementary Material. After manually tracing the brain, the skull-stripped MRI data were preprocessed using BRAINS2 (Brain Research: Analysis of Images, Networks and Systems), a locally developed software program described elsewhere (Magnotta *et al*., 2002). The T1-weighted images were spatially standardized by reorienting the horizontal plane to be parallel to the anterior commissure–posterior commissure line and perpendicular to the interhemispheric fissure. Data were resampled to 1.02 mm^3 voxels. The FreeSurfer software package (http://surfer.nmr.mgh.harvard.edu/), which has been validated and described in detail elsewhere (Dale, Fischl, and Sereno, 1999; Fischl, Sereno, and Dale, 1999; Fischl, Liu, and Dale, 2001) was used to delineate the cortical mantle and parcellate it based on the Desikan–Killiany atlas (Desikan *et al*., 2006). In brief, the cortical mantle was determined by segmenting white matter, tessellating the surface representation along the gray–white matter junction, and inflating until the pial surface is approximated. The gray–white matter and the pial surface representations were then refined based on intensity and continuity information using a deformable surface algorithm. For each vertex on the tessellated surfaces, cortical thickness was calculated based on the average of the shortest distance from pial surface to the gray/white surface and vice versa (Fischl and Dale, 2000). All data were then registered to a common surface-based template using a non-rigid spherical averaging method that aligns cortical folding patterns to match homologous structures (Fischl *et al*., 1999). Using a probabilistic labeling algorithm that relies on gyral and sulcal information, the cortex was parcellated into anatomical regions of interest (ROIs) (Fischl *et al*., 2004; Desikan *et al*., 2006) and projected back into each subject's native space. Volumetric measures reported in this study were derived from this automated parcellation procedure.

ROIs

The FreeSurfer parcellations were used to derive anatomical ROIs for this study, including: vmPFC, ACC, DLPFC, ventral visual stream and dorsal visual stream. See Figure 1 for anatomical delineation of ROIs. The vmPFC is composed of two regions, the medial orbitofrontal cortex (mOFC) and lateral orbitofrontal cortex (lOFC). The mOFC is composed of the straight gyrus on the OFC surface and a sector of the medial wall of the prefrontal cortex anterior to the cingulate gyrus. The lOFC contains the rest of the OFC, excluding the sector lateral to the lateral orbital sulcus. The ACC includes a rostral and caudal division, (rACC and cACC, respectively). The DL PFC is composed of all parcels that encompass the inferior and middle frontal gyrus. The superior frontal gyrus was excluded from the vmPFC and the DL PFC ROIs because it contains both medial and lateral components. The ventral visual stream includes the lateral occipital, fusiform and inferior temporal regions. The dorsal visual stream includes the inferior and superior parietal cortices along with the lateral occipital region. The anatomical boundaries of these regions and the intraclass correlation coefficient describing the correlation of automated and manual parcellation methods for each region are reported elsewhere (Desikan *et al*., 2006). The proportional gray matter volume of the ROIs relative to total cortex volume was computed and used as the dependent measure in regression analyses.

Cortical thickness analysis

Cortical thickness was calculated using FreeSurfer. These thickness measures were smoothed with a 25-mm full-width at half-maximum (FWHM) Gaussian kernel along the contour of the surface, respecting the cortical gyrification. A 15-mm FWHM Gaussian kernal was also used and is presented as Supplementary Material. The smoothed thickness data for each subject were imported into Matlab (http://www.mathworks.com), projected onto FreeSurfer's template brain, and used in vertex-wise regression analyses.

Fig. 1 FreeSurfer ROIs. This figure shows the regions of interest used in the study, including the vmPFC and anterior cingulate cortex in orange/red, the DL PFC in green, the ventral visual stream in blue and the dorsal visual stream in purple.

Statistical analysis

Regression analyses were performed using the ROI volumes or cortical thickness as the dependent measures. For each dependent measure, three separate regression analyses were performed: (i) a combined analysis of A.P. and S.M. with all the comparison subject data; (ii) an analysis of S.M. and her comparison group data; and (iii) an analysis of A.P. and her comparison data. In the combined analysis of S.M. and A.P., separate regressors were used for each subject and control group at each time point, averaging the differences between SM and respective control group data across time points and adjusting the denominator of the test statistic to account for the repeated measures of S.M. The regression model for S.M. and her comparison groups also used separate regressors at each time point. Again, as the three data points for S.M. reflected repeated measures of the same subject, the statistical test between S.M. and her controls entailed averaging the difference between S.M. and control group data across time points and adjusting the denominator of the statistical test to reflect the comparison of a single subject to a group. In the analysis of A.P., reference cell coding was used in the regression model to indicate subject group (lesion or control subject), allowing for independent sample *t*-tests between A.P. and her control group. Thus, all analyses assumed fixed effects using only within-group between-subject variance of the controls for the residual error estimates of the test statistics. All results were thresholded at $P < 0.05$, uncorrected. This relatively lenient threshold was decided in advance as there were very specific *a priori* hypotheses and in consideration of the practical matter that there were only two target subjects, a necessary limitation based on the rarity of isolated bilateral amygdala lesions. To reduce the risk of a type 1 error (falsely positive results) only regional findings that were consistent in S.M. and A.P. individually as well as in the combined analysis were considered positive findings. Moreover, the directionality of the finding had to match in terms of both subjects having either increased or decreased thickness of a given region. There has been considerable discussion in the literature on how best to compare case–studies to a control group, and our approach is justified provided that the mean of the control group is in fact a good estimate of the normal population mean; given our exceptionally large control group sample size, we believe this to be the case.

RESULTS

Table 2 displays the volumetric data of a combined analysis comparing S.M. and A.P. to their respective comparison groups along with analyses of S.M. and A.P. individually. S.M.s values reflect the average of the data acquired at three time points. A preliminary analysis examined whether global differences in brain volume existed in the lesion patients as compared to their respective controls. A significant decrease in total brain volume and total cerebral cortex volume was noted in S.M., while A.P. was within the normal range. When total cerebral cortex gray matter volume was taken as a percentage of brain volume, it did not differ from the comparison groups in S.M. or A.P., suggesting that while overall brain volume was decreased in S.M., there was not a disproportionate loss of cerebral cortex tissue. Thus, as is standardly done to account for differences in overall brain size, all regional analyses used the ratio of ROI volume to total cerebral cortex gray matter volume (e.g. vmPFC volume/total cortex volume) for combined and individual analyses.

ROI-based analyses demonstrated a proportional increase in vmPFC volume in a combined analysis of S.M. and A.P. relative to the comparison subjects. S.M. had a significantly higher proportion of cerebral cortex volume occupied by the vmPFC and a significant proportional reduction in ventral visual stream volume. There were no significant volumetric differences observed in A.P. relative to her comparison group. The dorsal visual stream and the DL PFC regions were included as 'control' regions to assess specificity of morphometric sequelae. These regions are sparsely connected to the amygdala and normal morphology was hypothesized. There were no differences between lesion and control subjects for either region that approached significance in the combined or individual analyses.

Table 2 Volumetric data

Region	A.P.	A.P. controls (SD)	*t*-value	S.M.	S.M. controls (SD)	*t*-value	A.P._S.M.	Controls (SD)	*t*-value
TBV	1286	1417 (135)	−0.96	970	1370 (132)	**−3.01****	1128	1394 (134)	**−2.78***
CCx	462	484 (43.8)	−0.50	313	444 (41)	**−3.16****	387	464 (42.6)	**−2.53***
CCx/TBV	35.9%	34.2% (1.3%)	1.27	32.2%	32.5% (1.3%)	−0.21	34.0%	33.3% (1.33%)	0.76
vmPFC	5.66%	5.41% (0.29%)	0.85	6.2%	5.37% (0.42%)	**2.07***	5.95%	5.39% (0.36%)	**2.20***
ACC	1.93%	1.78% (0.21%)	0.69	1.65%	1.79% (0.21%)	−0.65	1.79%	1.78% (0.21%)	0.03
Ventral visual stream	14.4%	13.9% (0.73%)	0.61	12.3%	14.2% (0.75%)	**−2.52***	13.3%	14.1% (0.74)	−1.39
DL PFC	14.10%	14.79% (0.77%)	−0.88	14.4%	14.5% (0.70%)	−1.91	14.23%	14.64% (0.74)	−0.78
Dorsal visual stream	17.40%	16.41% (0.64%)	1.54	16.0%	16.8% (0.81)	−0.95	16.7%	16.6 (0.73)	0.20

All regional volumetric measures are taken as a percentage of total cerebral cortex volume. Absolute volumes are in cubic centimeters. Values for SM represent an average of three time points.

*Significant to $P < 0.05$, **Significant to $P < 0.01$, Significant results are in bold.

Analysis of the cortical thickness data in a combined analysis of S.M. and A.P. relative to comparison groups revealed a significant increase in cortical thickness in the vmPFC and ACC bilaterally, compatible with our hypothesis. Analysis of individual cortical thickness data showed that S.M. had significantly increased thickness in a small region of the left anterior vmPFC and right anterior cingulate, while A.P. had increased vmPFC thickness bilaterally along with increased left ACC thickness. The combined analysis of S.M. and A.P. also showed decreased cortical thickness in the anteromesial temporal lobe of the ventral visual stream, a region near the amygdala, along with a very small region of right occipital lobe. The anteromesial temporal region was thin bilaterally in S.M. and on the left in A.P. in individual analyses.

A few significant findings were present in one of the subjects or one of the analyses that did not meet the full criteria for a positive finding (present in both subjects individually and in the combined analysis). These occurred in non-hypothesized regions. In the combined analysis this included increased thickness in the superior frontal gyrus bilaterally, left middle and inferior temporal gyrus and right lateral orbital frontal gyrus. Decreased thickness was seen in the superior frontal sulcus. In S.M., increased cortical thickness was seen in the left posterior cingulate, right precuneus, portions of the inferior parietal cortex, bilaterally, left postcentral gyrus and right lateral orbital and prefrontal cortex. Decreased thickness in S.M. was seen in the right superior parietal cortex and right premotor cortex. In A.P. increased cortical thickness included the left DLPFC, left middle and superior temporal gyrus, right superior frontal cortex and right lateral orbital frontal cortex. Decreased cortical thickness was seen in the left precuneus. Refer to Figures 2A–C for cortical thickness results (also see Supplementary Material for the same analysis with a smoothing kernel of 15).

DISCUSSION

The aim of this study was to examine whether long-standing developmental bilateral amygdala lesions were associated with alterations in cerebral cortex morphology in densely connected regions, namely the vmPFC, ACC, and ventral visual stream. Two women with rare bilateral amygdala lesions, S.M. and A.P., were used in the study and MRI data was analyzed relative to matched comparison groups. Compatible with the hypothesis, a combined analysis of S.M. and A.P. showed increased proportional volume of the vmPFC and increased thickness of the vmPFC bilaterally, along with the ACC. Decreased cortical thickness was observed in the anteromesial temporal lobes of the ventral visual stream. Analyzed individually, S.M. showed a significant proportional increase in vmPFC volume. There was increased thickness in the medial PFC (a sector of the vmPFC) and the adjacent ACC. There was a significant decrease in proportional volume and cortical thickness in the anterior ventral visual stream regions. A.P. had a normal volumetric profile with increased vmPFC thickness bilaterally and increased ACC thickness on the left side. There was also a small amount of cortical thinning observed in the anterior ventral visual stream. Of note, spatial correspondence between volumetric and cortical thickness findings in these analyses suggest that the latter, at least in part, may underlie the former.

In general, changes in cortical morphology in S.M. were more robust than in A.P. This included an overall decreased brain size with regionally specific morphological changes in regions consistent with our hypotheses based on amygdala connectivity. We showed that there was not a selective reduction in cortical volume in S.M. and other studies support the notion that differences in overall intracranial volume should not significantly impact measures of cortical thickness (Barnes *et al.*, 2010). There was no evidence of a more generalized degenerative process in S.M. (e.g. sulcal widening, increased cerebrospinal fluid around the brain) that would cause non-specific diffuse atrophy. We did not find any evidence for a progression in cortical morphological changes in S.M.s scans between the three different time points at which they were acquired, suggesting that, at least within the 12-year span of the scans, the longer duration of S.M.s lesion did not contribute to the larger effects on cortical volume and thickness that we report here. A more plausible explanation for S.M.s larger effects as compared to AP may instead be that S.M.s lesions are considerably more extensive, encompassing the entire amygdala with some cortical involvement in the adjacent entorhinal cortex, whereas A.P.s lesion occupies only about half of the amygdala's volume.

Volumetric and thickness differences were observed in both directions (increase *vs* decrease). The bi-directionality of our findings are not unexpected considering the developmental nature of the amygdala lesions. Developmental de-afferantation lesions have been noted to be associated with thicker cortex. For instance, the visual cortices are significantly thicker with early-onset blindness relative to control and late-onset blindness groups, presumably secondary to reduced pruning of synapses (Jiang *et al.*, 2009). The effect that de-afferentation has on cortical thickness likely depends on the maturity of the cortical region in question at the time of lesion onset. In the current study, we cannot specify the time of lesion onset in the two target subjects but amygdala lesions resulting from Urbach–Wiethe disease typically form around the age 10 years in most individuals (Aroni *et al.*, 1998; Staut and Naidich, 1998; Appenzeller *et al.*, 2006). This makes it likely that at the time of lesion onset the visual cortices had undergone synaptic pruning and achieved adult levels of cortical thickness (Huttenlocher and de Courten, 1987), whereas the prefrontal cortex may have been relatively immature, with pruning typically occurring later in adolescence (Huttenlocher and Dabholkar, 1997; Shaw *et al.*, 2008). With these cortical maturation profiles in mind, it would appear that the lesion may have occurred after a critical period of ventral visual stream development and before

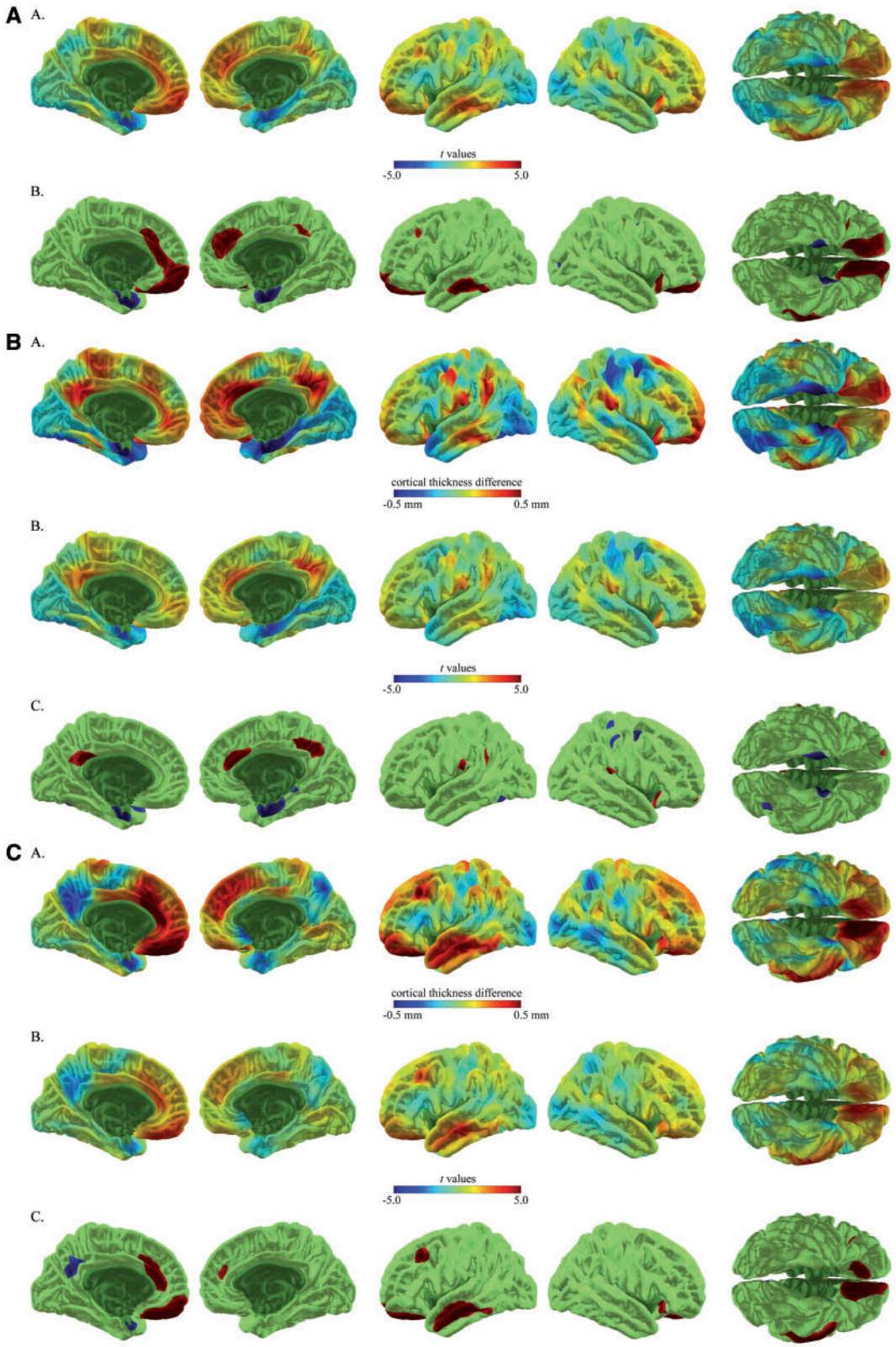

Fig. 2 Cortical thickness results for S.M. and A.P., as compared to matched control subjects, are presented in **A**–**C**. Results are rendered on the cortical surface of an average brain. (A) The combined analysis of S.M. and A.P. compared to controls. For this panel, row A shows the *t*-values associated with cortical thickness differences and row B shows the thresholded *t*-values at $P < 0$ .05 (uncorrected), [$t(108) = 1.99$]. (B and C) Individual comparisons of S.M. and A.P. relative to their comparison groups. For these panels, row A shows the magnitude of cortical thickness differences in millimeters, row B shows the *t*-values associated with these differences and row C shows the thresholded *t*-values at $P < 0$ .05 (uncorrected), [$t(56) = 2.01$ and $t(52) = 2.01$, respectively]. For all panels, positive *t*-values (warm end of the color spectrum) indicate where amygdalae lesion subjects have increased cortical thickness, while negative *t*-values (cool end of the color spectrum) indicate decreased cortical thickness.

the same period in the vmPFC/ACC regions. It is also possible that the ACC and vmPFC have greater capacity for structural reorganization and the increased thickness reflects plasticity.

However, previous work with these subjects involving a decision making task suggests that medial prefrontal cortex function is abnormal and so is behavioral performance on the task (Hampton *et al.*, 2007). This would suggest that compensation, if present, is suboptimal.

Focal lesions selectively involving the amygdala are extremely rare with only a few studies documenting such cases (Adolphs and Tranel, 1999; Siebert *et al.*, 2003; Thornton *et al.*, 2008). Such cases provide a unique and highly valuable model for research on neuropsychiatric conditions associated with amygdala dysfunction, including: autism, depression, post-traumatic stress disorder, anxiety, psychopathy and schizophrenia, among others. Each of these disorders has been associated with abnormal amygdala volume and altered cerebral cortex morphology. It remains unclear to what extent these structural differences in the cerebral cortex are: (i) primary, and directly related to the underlying mechanisms of the disease; (ii) are located downstream from an aberrant region; or (iii) represent a compensatory process. By demonstrating altered cerebral cortex structure in response to isolated amygdala lesions, the present study underscores the need for future studies of structural differences associated with these disorders to consider on a network perspective. Using structural neuroimaging in combination with the lesion method is one way to begin to understand the dynamic and integrative process of brain development and plasticity following localized brain damage.

It is important to be cautious in drawing conclusions from two subjects, and our ability to work with larger sample sizes is limited by the rarity of such presentations. Lesion studies in animals will be critical to confirm these findings and elaborate details regarding how early- *vs* late-onset lesions differentially impact cerebral cortex morphology. This work will complement ongoing studies showing altered functional changes in connected cortical regions of rats and monkeys (Gerrits *et al.*, 2006; Machado *et al.*, 2008). Despite the small sample size, this study provides the first evidence that amygdala lesions in humans impact the morphology of anatomically and functionally connected cortical regions, thus complementing previous work demonstrating altered functional activity in these connected regions.

SUPPLEMENTARY DATA

Supplementary data are available at *SCAN* online.

Conflict of Interest

None declared.

REFERENCES

Adolphs, R., Spezio, M. (2006). Role of the amygdala in processing visual social stimuli. *Progress in Brain Research*, *156*, 363–78.

Adolphs, R., Tranel, D. (1999). Intact recognition of emotional prosody following amygdala damage. *Neuropsychologia*, *37*(11), 1285–92.

Adolphs, R., Tranel, D., Damasio, H., Damasio, A. (1994). Impaired recognition of emotion in facial expressions following bilateral damage to the human amygdala. *Nature*, *372*(6507), 669–72.

Adolphs, R., Tranel, D., Damasio, H., Damasio, A.R. (1995). Fear and the human amygdala. *Journal of Neuroscience*, *15*(9), 5879–91.

Aggleton, J. (2000). *The amygdala: a functional analysis*. New York: Oxford University Press, pp. 31–115.

Amaral, D.G., Behniea, H., Kelly, J.L. (2003). Topographic organization of projections from the amygdala to the visual cortex in the macaque monkey. *Neuroscience*, *118*(4), 1099–120.

Amaral, D.G., Price, J.L. (1984). Amygdalo-cortical projections in the monkey (Macaca fascicularis). *The Journal of Comparative Neurology*, *230*(4), 465–96.

Appenzeller, S., Chaloult, E., Velho, P., et al. (2006). Amygdalae calcifications associated with disease duration in lipoid proteinosis. *Journal of Neuroimaging*, *16*(2), 154–6.

Aroni, K., Lazaris, A.C., Papadimitriou, K., Paraskevakou, H., Davaris, P.S. (1998). Lipoid proteinosis of the oral mucosa: case report and review of the literature. *Pathology, Research and Practice*, *194*(12), 855–9.

Barbas, H., De Olmos, J. (1990). Projections from the amygdala to basoventral and mediodorsal prefrontal regions in the rhesus monkey. *The Journal of Comparative Neurology*, *300*(4), 549–71.

Barnes, J., Ridgway, G.R., Bartlett, J., et al. (2010). Head size, age and gender adjustment in MRI studies: a necessary nuisance? *Neuroimage*, *53*(4), 1244–55.

Bechara, A., Damasio, H., Damasio, A.R. (2003). Role of the amygdala in decision-making. *Annals of the New York Academy of Science*, *985*, 356–69.

Buchanan, T.W., Tranel, D., Adolphs, R. (2009). The human amygdala in social function. In: Whalen, P.W., Phelps, L., editors. *The Human Amygdala*. New York: Oxford University Press, pp. 289–20.

Carmichael, S.T., Price, J.L. (1995). Limbic connections of the orbital and medial prefrontal cortex in macaque monkeys. *The Journal of Comparative Neurology*, *363*(4), 615–41.

Cohen, M.X., Elger, C.E., Weber, B. (2008). Amygdala tractography predicts functional connectivity and learning during feedback-guided decision-making. *Neuroimage*, *39*(3), 1396–407.

Dale, A.M., Fischl, B., Sereno, M.I. (1999). Cortical surface-based analysis. I. Segmentation and surface reconstruction. *Neuroimage*, *9*(2), 179–94.

Desikan, R.S., Segonne, F., Fischl, B., et al. (2006). An automated labeling system for subdividing the human cerebral cortex on MRI scans into gyral based regions of interest. *Neuroimage*, *31*(3), 968–80.

Fischl, B., Dale, A.M. (2000). Measuring the thickness of the human cerebral cortex from magnetic resonance images. *Proceedings of the National Academy of Sciences of the United States of America*, *97*(20), 11050–5.

Fischl, B., Liu, A., Dale, A.M. (2001). Automated manifold surgery: constructing geometrically accurate and topologically correct models of the human cerebral cortex. *IEEE Transactions on Medical Imaging*, *20*(1), 70–80.

Fischl, B., Sereno, M.I., Dale, A.M. (1999). Cortical surface-based analysis. II: Inflation, flattening, and a surface-based coordinate system. *Neuroimage*, *9*(2), 195–207.

Fischl, B., van der Kouwe, A., Destrieux, C., et al. (2004). Automatically parcellating the human cerebral cortex. *Cerebral Cortex*, *14*(1), 11–22.

Freese, J.L., Amaral, D.G. (2005). The organization of projections from the amygdala to visual cortical areas TE and V1 in the macaque monkey. *The Journal of Comparative Neurology*, *486*(4), 295–317.

Freese, J.L., Amaral, D.G. (2006). Synaptic organization of projections from the amygdala to visual cortical areas TE and V1 in the macaque monkey. *The Journal of Comparative Neurology*, *496*(5), 655–67.

Gaffan, D., Murray, E.A., Fabre-Thorpe, M. (1993). Interaction of the amygdala with the frontal lobe in reward memory. *European Journal of Neuroscience*, *5*(7), 968–75.

Gerrits, M.A., Wolterink, G., van Ree, J.M. (2006). Cerebral metabolic consequences in the adult brain after neonatal excitotoxic lesions of the amygdala in rats. *European Neuropsychopharmacology*, *16*(5), 358–65.

Ghashghaei, H.T., Hilgetag, C.C., Barbas, H. (2007). Sequence of information processing for emotions based on the anatomic dialogue between prefrontal cortex and amygdala. *Neuroimage*, *34*(3), 905–23.

Hampton, A.N., Adolphs, R., Tyszka, M.J., O'Doherty, J.P. (2007). Contributions of the amygdala to reward expectancy and choice signals in human prefrontal cortex. *Neuron*, *55*(4), 545–55.

Holmes, C.J., Hoge, R., Collins, L., Woods, R., Toga, A.W., Evans, A.C. (1998). Enhancement of MR images using registration for signal averaging. *Journal of Computer Assisted Tomography*, *22*(2), 324–333.

Huttenlocher, P.R., Dabholkar, A.S. (1997). Regional differences in synaptogenesis in human cerebral cortex. [Comparative Study Research Support, U.S. Gov't, P.H.S.]. *The Journal of Comparative Neurology*, *387*(2), 167–78.

Huttenlocher, P.R., de Courten, C. (1987). The development of synapses in striate cortex of man. *Human Neurobiology*, *6*(1), 1–9.

Iwai, E., Yukie, M. (1987). Amygdalofugal and amygdalopetal connections with modality-specific visual cortical areas in macaques (Macaca fuscata, M. mulatta, and M. fascicularis). *The Journal of Comparative Neurology*, *261*(3), 362–87.

Jiang, J., Zhu, W., Shi, F., et al. (2009). Thick visual cortex in the early blind. [Research Support, Non-U.S. Gov't]. *The Journal of Neuroscience: the official Journal of the Society for Neuroscience*, *29*(7), 2205–11.

Johansen-Berg, H., Gutman, D.A., Behrens, T.E., et al. (2008). Anatomical Connectivity of the Subgenual Cingulate Region Targeted with Deep Brain Stimulation for Treatment-Resistant Depression. *Cerebral Cortex*, *18*(6), 1374–83.

Machado, C.J., Snyder, A.Z., Cherry, S.R., Lavenex, P., Amaral, D.G. (2008). Effects of neonatal amygdala or hippocampus lesions on resting brain metabolism in the macaque monkey: a microPET imaging study. *Neuroimage*, *39*(2), 832–46.

Magnotta, V.A., Harris, G., Andreasen, N.C., O'Leary, D.S., Yuh, W.T., Heckel, D. (2002). Structural MR image processing using the BRAINS2 toolbox. *Computerized Medical Imaginging and Graph*, *26*(4), 251–64.

Morecraft, R.J., McNeal, D.W., Stilwell-Morecraft, K.S., et al. (2007). Amygdala interconnections with the cingulate motor cortex in the rhesus monkey. *The Journal of Comparative Neurology*, *500*(1), 134–65.

Pezawas, L., Meyer-Lindenberg, A., Drabant, E.M., et al. (2005). 5-HTTLPR polymorphism impacts human cingulate-amygdala interactions: a genetic susceptibility mechanism for depression. *Nature Neuroscience*, *8*(6), 828–34.

Porrino, L., Crane, A., Goldman Rakic, P. (1981). Direct and indirect pathways from the amygdala to the frontal lobe in rhesus monkeys. *The Journal of Comparative Neurology*, *198*(1), 121–36.

Rudrauf, D., David, O., Lachaux, J.P., et al. (2008). Rapid interactions between the ventral visual stream and emotion-related structures rely on a two-pathway architecture. *Journal of Neuroscience*, *28*(11), 2793–803.

Shaw, P., Kabani, N.J., Lerch, J.P., et al. (2008). Neurodevelopmental trajectories of the human cerebral cortex. *Journal of Neuroscience*, *28*(14), 3586–94.

Siebert, M., Markowitsch, H., Bartel, P. (2003). Amygdala, affect and cognition: evidence from 10 patients with Urbach-Wiethe disease. *Brain*, *126*(12), 2627.

Staut, C.C., Naidich, T.P. (1998). Urbach-Wiethe disease (Lipoid proteinosis). *Pediatric Neurosurgery*, *28*(4), 212–4.

Stefanacci, L., Amaral, D.G. (2000). Topographic organization of cortical inputs to the lateral nucleus of the macaque monkey amygdala: a retrograde tracing study. *The Journal of Comparative Neurology*, *421*(1), 52–79.

Stefanacci, L., Amaral, D. (2002). Some observations on cortical inputs to the macaque monkey amygdala: an anterograde tracing study. *The Journal of Comparative Neurology*, *451*(4), 301–23.

Stein, J.L., Wiedholz, L.M., Bassett, D.S., et al. (2007). A validated network of effective amygdala connectivity. *Neuroimage*, *36*(3), 736–45.

Thornton, H., Nel, D., Thornton, D., van Honk, J., Baker, G., Stein, D. (2008). The neuropsychiatry and neuropsychology of lipoid proteinosis. *Journal of Neuropsychiatry and Clinical Neurosciences*, *20*(1), 86–92.

Tranel, D., Hyman, B.T. (1990). Neuropsychological correlates of bilateral amygdala damage. *Archives of Neurology*, *47*(3), 349–55.

Tranel, D., Gullickson, G., Koch, M., Adolphs, R. (2006). Altered experience of emotion following bilateral amygdala damage. *Cognit Neuropsychiatry*, *11*(3), 219–32.

Turner, B.H., Mishkin, M., Knapp, M. (1980). Organization of the amygdalopetal projections from modality-specific cortical association areas in the monkey. *The Journal of Comparative Neurology*, *191*(4), 515–43.

Vuilleumier, P., Driver, J. (2007). Modulation of visual processing by attention and emotion: windows on causal interactions between human brain regions. *Philosophical Transactions of the Royal Society of London B: Biological Sciences*, *362*(1481), 837–55.

Vuilleumier, P., Richardson, M.P., Armony, J.L., Driver, J., Dolan, R.J. (2004). Distant influences of amygdala lesion on visual cortical activation during emotional face processing. *Nature Neurosciences*, *7*(11), 1271–8.

Whalen, P., Phelps, E. (2009). *The Human Amygdala*. The Guilford Press.